

Efficient finite element analysis using graph-theoretical force method; rectangular plane stress and plane strain serendipity family elements

Ali Kaveh / Mohammad Sajjad Massoudi / Mohammad Javad Massoudi

Received 2012-09-19, accepted 2013-10-04

Abstract

Formation of a suitable null basis for equilibrium matrix is the main part of finite elements analysis via force method. For an optimal analysis, the selected null basis matrices should be sparse and banded corresponding to produce sparse, banded and well-conditioned flexibility matrices. In this paper, an efficient method is developed for the formation of null bases of finite element models (FEMs) consisting of rectangular plane stress and plane strain serendipity family elements, corresponding to highly sparse and banded flexibility matrices. This is achieved by associating special graphs with the FEM and selecting appropriate subgraphs and forming the self-equilibrating systems (SEs) on these subgraphs. The efficiency of the present method is illustrated through three examples.

Keywords

Finite elements · Force method · Null basis · Flexibility matrix · Graph theory · Plane stress · Plane strain · Rectangular elements · Serendipity family elements

1 Introduction

The force method of structural analysis in which the member forces are used as unknowns is appealing to engineers since the properties of members of a structure most often depend on the member forces rather than joint displacements. This method was used extensively until 1960. The advent of the digital computer and the amenability of the displacement method for computation attracted most researchers. As a result, the force method and some of the advantages it offers in non-linear analysis and optimization has been neglected.

Five different approaches are adopted for the force method of structural analysis, classified as:

- 1 Topological force methods,
- 2 Graph theoretical methods,
- 3 Algebraic force methods,
- 4 Mixed algebraic-combinatorial force methods,
- 5 Integrated force method.

Topological methods have been developed by Henderson [1] Maunder [2] and Henderson and Maunder [3] for rigid-jointed skeletal structures. Graph theoretical methods based on cycle bases of the graph models are due to Kaveh [4, 5]. These methods are generalized to cover different types of skeletal structures such as rigid-jointed frames, pin-jointed planar trusses and ball-jointed space trusses in [6, 7].

Algebraic methods have been developed by Denke [8], Robinson [9], Topçu [10], Kaneko et al. [11], and Soyer and Topçu [12]. Mixed algebraic-topological methods have been used by Gilbert et al. [13] Coleman and Pothen [14, 15], Pothen [16], and Heath et al. [17]. The integrated force method has been developed by Patnaik [18, 19], in which the equilibrium and compatibility conditions are satisfied simultaneously in terms of the element force variables [20].

Recently applications of the graph theory methods are extended to two classes of finite element models. The first class takes the element forces along the edges of the elements [21–23] and in the second class the element forces are concentrated at

Ali Kaveh

Centre of Excellence for Fundamental Studies in Structural Engineering, University of Science and Technology, Narmak, P.O. Box 16846-13114, Iran
e-mail: alikaveh@iust.ac.ir

Mohammad Sajjad Massoudi

Mohammad Javad Massoudi

Centre of Excellence for Fundamental Studies in Structural Engineering, University of Science and Technology, Narmak, P.O. Box 16846-13114, Iran

the mid-edge of the edges of the elements [24, 25]. In this paper, an efficient method is developed for the formation of null bases for finite element models comprising of rectangular plane stress and plane strain serendipity family elements leading to highly sparse and banded flexibility matrices, and can be used for optimal finite element analysis by the force method. This is achieved by associating a special graph to the finite element model and selecting subgraphs (known as γ -cycles [6]) for the formation of localized self-equilibrating stress systems (null vectors). Their numerical values are calculated by an algebraic process. The efficiency and accuracy of the present method is illustrated through simple examples.

2 Formulation of Force Method

Consider a discrete or discretized structure which is statically indeterminate. The m -dimensional vector \mathbf{r} contains independent element (member) forces, and an n -dimensional vector \mathbf{p} denotes the nodal loads. The equilibrium equations of the structure can then be expressed as:

$$\mathbf{A}\mathbf{r} = \mathbf{p} \quad (1)$$

where \mathbf{A} is an $n \times m$ equilibrium matrix. Assuming stability for the structure, the equilibrium matrix will have full rank, i.e. $t = m - n > 0$, $\text{rank}(\mathbf{A}) = n$.

Also the member forces can be written as the sum of the particular and complementary solutions, where \mathbf{q} is the t -dimensional vector of the redundant forces.

$$\mathbf{r} = \mathbf{B}_0\mathbf{p} + \mathbf{B}_1\mathbf{q} \quad (2)$$

\mathbf{B}_0 and \mathbf{B}_1 have m rows and n , and t columns, respectively. Pre-multiplying both sides of Eq. (2) by \mathbf{A} and using Eq. (1) lead to

$$\mathbf{A}\mathbf{B}_0 = \mathbf{I} \quad (3)$$

$$\mathbf{A}\mathbf{B}_1 = \mathbf{0} \quad (4)$$

Here, \mathbf{B}_0 and \mathbf{B}_1 are not unique for a structure and many of such matrices can be formed. \mathbf{B}_1 is called static basis or self-stress matrix. This basis is known as null basis in mathematics and each column of the null basis matrix is known as a null vector. The null space and null vectors are mathematical counterparts of the complementary solution space and self-equilibrating systems, respectively.

Minimizing the complementary potential energy subjected to the constraint as in Eq. (1) requires \mathbf{r} to minimize the quadratic form

$$\text{minimize} \left(\frac{1}{2} \mathbf{r}^t \mathbf{F}_m \mathbf{r} \right) \quad (5)$$

Here, \mathbf{F}_m is a $m \times m$ block diagonal matrix known as the unassembled flexibility matrix containing the flexibility matrices of the elements of a structure in its block diagonal entries. Coupling Eq. (5) and Eq. (2) results in

$$\mathbf{q} = - \left(\mathbf{B}_1^t \mathbf{F}_m \mathbf{B}_1 \right)^{-1} \left(\mathbf{B}_1^t \mathbf{F}_m \mathbf{B}_0 \right) \mathbf{p} \quad (6)$$

According to Eq. (6) by solving a set of equations, redundant forces can be found.

After the determination of the member forces, using the load-displacement relationship for each member, one can write member distortion as

$$[\mathbf{u}] = [\mathbf{F}_m] [\mathbf{r}] = [\mathbf{F}_m] [\mathbf{B}_0 \ \mathbf{B}_1] \begin{bmatrix} \mathbf{p} \\ \mathbf{q} \end{bmatrix} \quad (7)$$

Using virtual work, nodal displacements can be calculated as

$$[\mathbf{v}_0] = [\mathbf{B}'_0] [\mathbf{u}] \quad (8)$$

Combining Eq. (7) and Eq. (8) leads to

$$\mathbf{v}_0 = \mathbf{B}'_0 \mathbf{F}_m \mathbf{B}_0 \mathbf{p} + \mathbf{B}'_0 \mathbf{F}_m \mathbf{B}_1 \mathbf{q} \quad (9)$$

Substituting Eq. (6) in Eq. (9) and using $\mathbf{D}_{ij} = \mathbf{B}'_i \mathbf{F}_m \mathbf{B}_j$ leads to

$$\mathbf{v}_0 = \left[\mathbf{D}_{00} - \mathbf{D}_{01} \mathbf{D}_{11}^{-1} \mathbf{D}_{10} \right] \mathbf{p} = \mathbf{F} \mathbf{p} \quad (10)$$

Therefore the overall flexibility matrix of structure is obtained as

$$\mathbf{F} = \mathbf{D}_{00} - \mathbf{D}_{01} \mathbf{D}_{11}^{-1} \mathbf{D}_{10} \quad (11)$$

For free vibration of linear structure without damping we have

$$\left[[\mathbf{K}] - \omega^2 [\mathbf{M}] \right] [\mathbf{v}_0] = \mathbf{0} \quad (12)$$

Obviously $\mathbf{K}\mathbf{v}_0 = \mathbf{p}$ and substituting Eq. (10) in Eq. (12) leads to

$$\left[[\mathbf{I}] - \omega^2 [\mathbf{M}] [\mathbf{F}] \right] [\mathbf{p}] = \mathbf{0} \quad (13)$$

Then the frequency equation of the system in the force method is obtained as

$$| [\mathbf{M}] [\mathbf{F}] - \lambda [\mathbf{I}] | = \mathbf{0} \quad \text{and} \quad \lambda = \frac{1}{\omega^2} \quad (14)$$

Efficiency of this analysis depends on the required time for the formation of the matrix $\mathbf{G} = \mathbf{B}'_1 \mathbf{F}_m \mathbf{B}_1$ and its characteristics, i.e. sparsity and bandedness together with its conditioning. For the formation of a well-structured matrix \mathbf{G} , one should select a well-structured \mathbf{B}_1 matrix.

Many algebraic procedures based on various matrix factorizations such as Gauss-Jordan elimination, LU , QR , LQ exist for the formation a null basis matrix \mathbf{B}_1 of an equilibrium matrix \mathbf{A} . Basic concept of these methods is described briefly in the following. Let matrix \mathbf{A} be partitioned using a column permutation matrix \mathbf{P} as below:

$$\mathbf{A}\mathbf{P} = [\mathbf{A}_1, \mathbf{A}_2] \quad (15)$$

Where \mathbf{A}_1 is a $n \times n$ non-singular matrix. Obviously matrix \mathbf{B}_1 can be written as

$$\mathbf{B}_1 = \mathbf{P} \begin{bmatrix} -\mathbf{A}_1^{-1} \mathbf{A}_2 \\ \mathbf{I} \end{bmatrix} \quad (16)$$

The complete description of algebraic force method can be found in Refs. [30, 31] and for brevity is not repeated in here.

3 Independent element forces and flexibility matrix of a two-dimensional rectangular element

For the generation of the equilibrium matrix \mathbf{A} of a FEM, a set of independent forces system should be defined and also their relations with the element nodal forces should be established [26].

In displacement method we have two forces at each node of the element. For an element with N nodes, $2 \times N$ nodal forces can be defined. Using three equilibrium equations, $2N - 3$ independent forces will remain. In other words, there are $2N - 3$ independent element forces in an element with N nodes. The nodal forces and element forces systems are shown in Fig. 1 for rectangular plane stress and plane strain serendipity family elements with various numbers of boundary nodes. For the higher order elements, the element forces system can be obtained with the same procedure.

These element forces can be related to the nodal forces for a rectangular element by a $(2N) \times (2N - 3)$ transformation matrix using Eq. (17) as

$$\mathbf{S} = \mathbf{TF} \quad (17)$$

Transformation matrix can be formed simply as

$(n_1, n_2) = \text{end nodes of element force } F_j$

For $i = 1 : N$

For $j = 1 : 2N - 3$

If $i == n_1$ $T(2i - 1, j) = m_{n_1 n_2}$ and $T(2i, j) = n_{n_1 n_2}$

If $i == n_2$ $T(2i - 1, j) = m_{n_2 n_1}$ and $T(2i, j) = n_{n_2 n_1}$

End

End

where x_i and y_i are the Cartesian coordinates of node i , $m_{ij} = \frac{x_i - x_j}{l_{ij}}$, $n_{ij} = \frac{y_i - y_j}{l_{ij}}$ are the direction cosines and l_{ij} is the length of the line between nodes i and j .

Formulation of a discrete element equivalent to the actual continuous structure is the first step in matrix structural analysis. For a linear system it can be assumed that the stresses σ are related to the forces \mathbf{F} by linear equation as

$$\sigma = \bar{\mathbf{c}}\mathbf{F} \quad (18)$$

The matrix $\bar{\mathbf{c}}$ represents a statically equivalent stress system due to the unit force \mathbf{F} . The flexibility matrix of an element can be written as

$$\mathbf{f}_m = \int_V \bar{\mathbf{c}}^t \boldsymbol{\varphi} \bar{\mathbf{c}} dV \quad (19)$$

The integration is taken over the area of the element, where $\boldsymbol{\varphi}$ is the matrix relating the stresses to strains $\boldsymbol{\varepsilon} = \boldsymbol{\varphi}\sigma$ in two dimensional problems [27]. The primary step in the formation of the flexibility matrix of an element is determining the matrix $\bar{\mathbf{c}}$. It is obvious that the i^{th} column of $\bar{\mathbf{c}}$ represents the resultant stresses due to unit element force \mathbf{F}_i in the force method and also stresses due to nodal forces \mathbf{S} is equal to the i^{th} column of \mathbf{T} utilizing the displacement method. Hence, we can form matrix $\bar{\mathbf{c}}$ using the stiffness properties of the rectangular element

using the displacement method. Now the flexibility matrix of the element in the force method is formed from Eq. (19) using Gauss numerical integration method with four Gauss points.

Therefore, each Type II minimal cycle corresponds to three null vectors which are calculated utilizing an algebraic method.

4 Graphs associated with finite element models

4.1 Basic graph theory definitions

A graph S consists of a set of elements, $N(S)$, called *nodes* and a set of elements, $M(S)$, called *members*, together with a relation of incidence which associates two distinct nodes with each member, known as its *ends*. Two nodes of a graph are called *adjacent* if these nodes are the end nodes of a member. A member is considered *incident* with a node if it is an end node of the member. The *degree* of a node is the number of members incident with that node. A *subgraph* S_i of a graph S is a graph for which $N(S_i) \subseteq N(S)$ and $M(S_i) \subseteq M(S)$, and each member of S_i has the same ends as in S . A *path* of S is a finite sequence $P_i = \{n_0, m_1, n_1, \dots, m_p, n_p\}$ whose terms are alternately distinct nodes n_i and distinct members m_i of S for $1 \leq i \leq p$, and n_{i-1} and n_i are the two ends of m_i . Two nodes n_i and n_j are said to be *connected* in S if there exists a path between these nodes. A *cycle* is a path $(n_0, m_1, n_1, \dots, m_p, n_p)$ for which $n_0 = n_p$ and $p \geq 3$; i.e. a cycle is a closed path. The cycles of a graph form a vector space known as the *cycle space*. The dimension of this space for a connected graph S is known as the *first Betti number*, $b_1(S) = M(S) - N(S) + 1$, of the graph, where $M(S)$ and $N(S)$ are the number of members and nodes of S , respectively. In order to transfer the topological property of a finite element model to the connectivity of a graph ten different graphs are introduced in [28, 29].

4.2 An interface graph

The interface graph of a finite element model denoted by IG (FEM) can easily be constructed for rectangular FEM using the following rules:

- 1 This graph contains all the nodes of the FEM.
- 2 With the all edges of an element of FEM, N graph members are associated. Therefore, in the interface of two elements, $2N$ -multiple members are presented.
- 3 For each element with N nodes, $2N-3$ members should be considered in the interface graph. Thus, $N-3 = (2N-3) - N$ diagonal members should be added. This graph for a quadratic and cubic FEM is shown in Fig. 2.

The member numbering of the interface graph should be performed according to the numbering of the FEM, taking into account the primary nodal numbering of a considered element in the model. Thus, for each rectangular element $2N-3$ members of the interface graph will be numbered sequentially according to the patterns which were illustrated in Fig. 1.

Element	Nodes number	Size of T	Nodal forces	Element forces	Element forces
Linear	$N = 4$	8×5	$S_{8 \times 1} = [S_1 \dots S_8]^T$	$F_{5 \times 1} = [F_1 \dots F_5]^T$	
Quadratic	$N = 8$	16×13	$S_{16 \times 1} = [S_1 \dots S_{16}]^T$	$F_{13 \times 1} = [F_1 \dots F_{13}]^T$	
Cubic	$N = 12$	24×21	$S_{24 \times 1} = [S_1 \dots S_{24}]^T$	$F_{21 \times 1} = [F_1 \dots F_{21}]^T$	
Quartic	$N = 16$	32×29	$S_{32 \times 1} = [S_1 \dots S_{32}]^T$	$F_{29 \times 1} = [F_1 \dots F_{29}]^T$	

Fig. 1. A set of rectangular serendipity family elements.

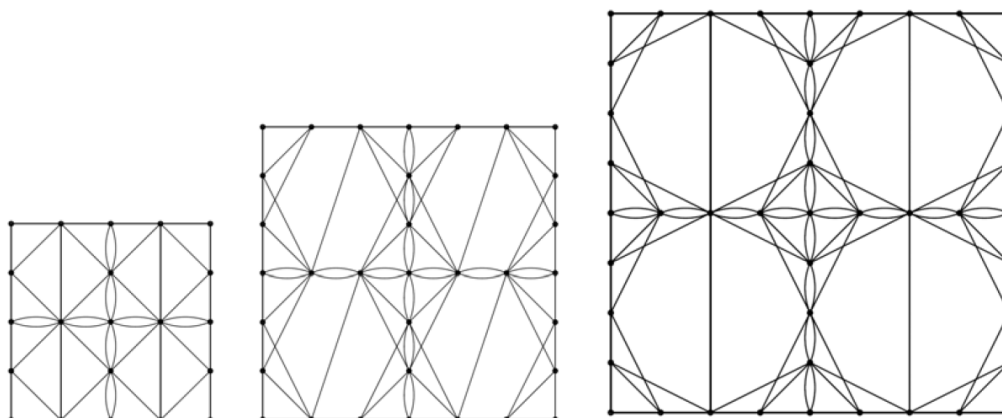


Fig. 2. A quadratic, cubic and quartic rectangular FEM with their interface graphs.

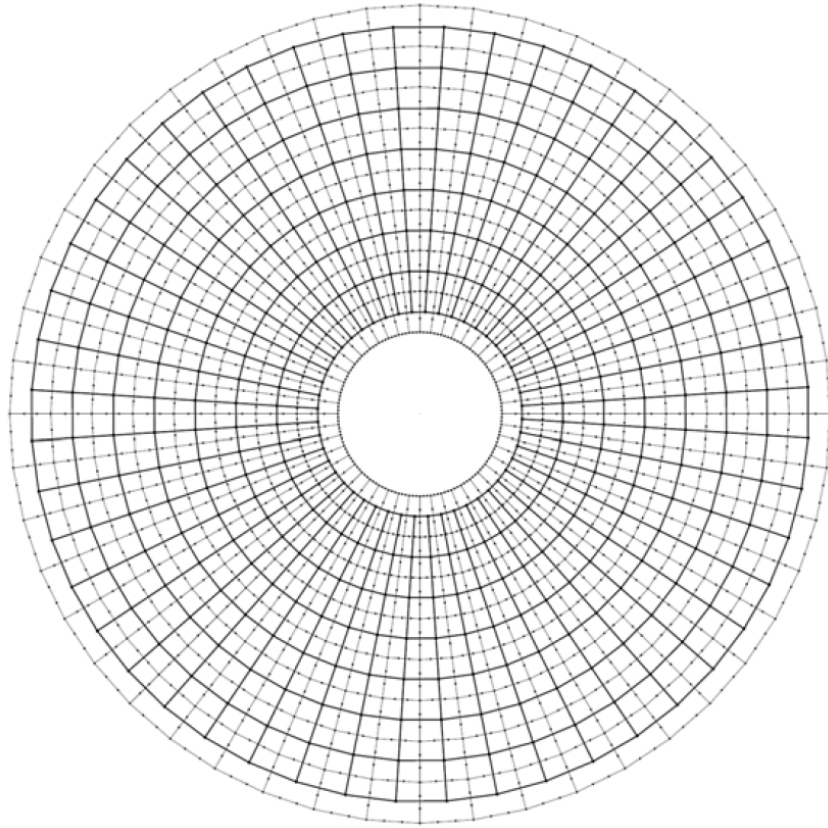


Fig. 3. A quadratic rectangular FEM with its natural associate graph (bold lines) for a circular plate.

4.3 Natural associate graph

The natural associate graph represented by $NAG(FEM)$ is constructed by the following rules:

- 1 Nodes of the $NAG(FEM)$ correspond to the elements of FEM.
- 2 For each pair of elements in FEM having $(N + 4)/4$ common nodes, one member is added between the corresponding two nodes in $NAG(FEM)$.

NAG can be constructed using the following procedure: One of the preliminary steps in FEM is defining the elements with their connected nodes. In this way the element connectivity matrix is constructed which contains the element-node incidence relationships. In the process of constructing the element connectivity matrix, another matrix which contains node-element incidence properties can be formed. This matrix is named the node connectivity matrix. Now using the element connectivity and the node connectivity matrices leads to an algorithm with complexity $O(n)$ for an efficient generation of NAG .

In order to recognize the adjacent elements to the n^{th} element which have $(N + 4)/4$ common nodes or one common face, first the connected nodes to the n^{th} element are identified from the element connectivity matrix. In the subsequent step using the node connectivity matrix, elements which have at least one common node with the n^{th} element are identified. Now it is convenient to seek for the adjacent elements in this reduced search space. A FEM and its corresponding NAG are illustrated in Fig. 3.

5 Pattern corresponding to the self-equilibrating systems

Considering Fig. 1, in order to find the patterns corresponding to the self-equilibrating systems, a rectangular element is simulated as a planar truss formed as the 1-skeleton of the rectangular element together with some diagonal members. This is possible since the independent element forces applied at in the nodes and are along the edges of the rectangular element. The statical indeterminacy of a planar truss with m members and n nodes is given as $\gamma(S) = m - 2n + 3$; therefore, the degree of statical indeterminacy (DSI) of the entire model supported in a statically determinate manner can be calculated with the same relationship as

$$DSI = (2N - 3) \times M - 2n + 3 \quad (20)$$

where M is the total number of elements, N is the number of nodes within an element and n is the total number of nodes of the FEM.

With the above simulation, the patterns of the self-equilibrating systems can be identified as follows:

5.1 Type I self-equilibrating systems

Each multiple member of the interface graph is a subgraph on which one self-equilibrating system can be generated. In other words, on a 2-multiple member numbered as (i, j) with the condition $(i < j)$, one self-equilibrating system can be constructed (extracted).

Each pair such as (i, j) for which $(i < j)$ corresponds to a null vector with their non-zero entries being located in rows i and j , and their numeric values are $(-1, 1)$, respectively. The member with bigger member number (j) is called the generator. These pairs are called Type I self-equilibrating systems

For a FEM we have $\frac{N}{4} \times M'$ self-equilibrating systems of Type I, where M' is the number of members of the associate graph of the model.

5.2 Type II self-equilibrating systems

There are other types of self-equilibrating systems which are extracted from two adjacent elements of FEM. In other words, for two adjacent elements with N nodes, the DSI can be calculated as:

$$\begin{aligned} DSI &= (2N - 3) \times M - 2n + 3 \\ \Rightarrow DSI &= (2N - 3) \times 2 - 2 \times (2N - \frac{N+4}{4}) + 3 = N - 7 \end{aligned} \quad (21)$$

$\frac{N}{4}$ self-equilibrating systems were generated as Type I systems. Thus the number of remaining self-equilibrating systems is

$$Type\ II = \frac{N}{2} - 1 - \frac{N}{4} = \frac{N}{4} - 1 \quad (22)$$

In other words, $\frac{N}{4} - 1$ SESs should be extracted from two adjacent elements. This number is equal to the number of internal nodes of the remaining subgraph after deleting the generators of SESs of Type I. For example, the remaining subgraphs for two adjacent cubic elements are shown in Fig. 4(a) in two directions. In this figure, the diagonal members are curved for better illustration. After deleting the generators corresponding to Type I SESs, the null vectors should be calculated from the remaining subgraph. These null vectors can easily be generated on the corresponding sub-structure utilizing an algebraic method. For instance, results SESs in horizontal direction are shown in Fig. 4(b).

In a FEM, the total number of Type II SESs can be calculated as:

$$Type\ II = M' \times \left(\frac{N}{4} - 1\right) \quad (23)$$

where M' is the number of members of the associate graph of the model and N is the number of nodes of an element.

The most important point in Type II self-equilibrating systems is to select an appropriate generator. In fact by eliminating these generators from graph S , the sub-structure of Type III SESs and the primary structure of the structure S must remain stable.

5.3 Type III self-equilibrating systems

Sub-structures which are topologically identical to the minimal cycles of the natural associate graph of FEM contains some Type I, II and one Type III self-equilibrating systems.

5.3.1 Type I minimal cycles of NAG(S)

These minimal cycles of the natural associate graph of the FEM pass through four elements which have one common node. Corresponding interface graph of these elements have n nodes and m edges for a FEM with N node elements.

$$m = 4 \times (2N - 3) \quad (24)$$

$$n = 4N - 4 \times \left(\frac{N+4}{4}\right) + 1 = 3 \times (N - 1) \quad (25)$$

Subsequently, the DSI of the interface graph is

$$\begin{aligned} DSI &= m - 2n + 3 \\ \Rightarrow DSI &= 4 \times (2N - 3) - 2 \times (3 \times (N - 1)) + 3 = 2N - 3 \end{aligned} \quad (26)$$

The N ($N = \frac{N}{4} \times M' = \frac{N}{4} \times 4$), SESs are Type I and there are $N - 4$, ($N - 4 = M' \times (\frac{N}{4} - 1) = 4 \times (\frac{N}{4} - 1)$), SESs of Type II.

$$DSI - (Type\ I \& II) = (2N - 3) - (N + (N - 4)) = 1 \quad (27)$$

Therefore, one independent SES should be extracted. This SES with eight members can be formed for any types of rectangular elements around the common node as is indicated bold in Fig. 5.

5.3.2 Type II minimal cycles of NAG(S)

Each minimal cycle that surrounds an opening is called the Type II minimal cycle. Such a cycle passes through M' , ($M' \geq 8$), finite elements and its corresponding interface graph has $(\frac{3N}{4} - 1) \times M'$ nodes and $M' \times (2N - 3)$ members. The DSI of subgraph is

$$\begin{aligned} DSI &= M' \times (2N - 3) - 2 \times \left(\frac{3N}{4} - 1\right) \times M' + 3 \\ \Rightarrow DSI &= M' \times \left(\frac{N}{2} - 1\right) + 3 \end{aligned} \quad (28)$$

that $\frac{N}{4} \times M'$ SESs of Type I and Type II = $M' \times \left(\frac{N}{4} - 1\right)$ SESs of Type II can be extracted.

$$\begin{aligned} DSI - Type\ I \& Type\ II &= M' \times \left(\frac{N}{2} - 1\right) \\ &- \left[M' \times \frac{N}{4} + M' \times \left(\frac{N}{4} - 1\right)\right] + 3 = 3 \end{aligned} \quad (29)$$

6 Selection of generators for SESs of Type II and Type III

The most important point in Type II and Type III self-equilibrating systems is to select appropriate generators. This is by eliminating these generators from graph S , the sub-structure of primary structure of the structure S must remain stable. To achieve this, the following rule for appropriate selection of generators of Type II SESs is suggested.

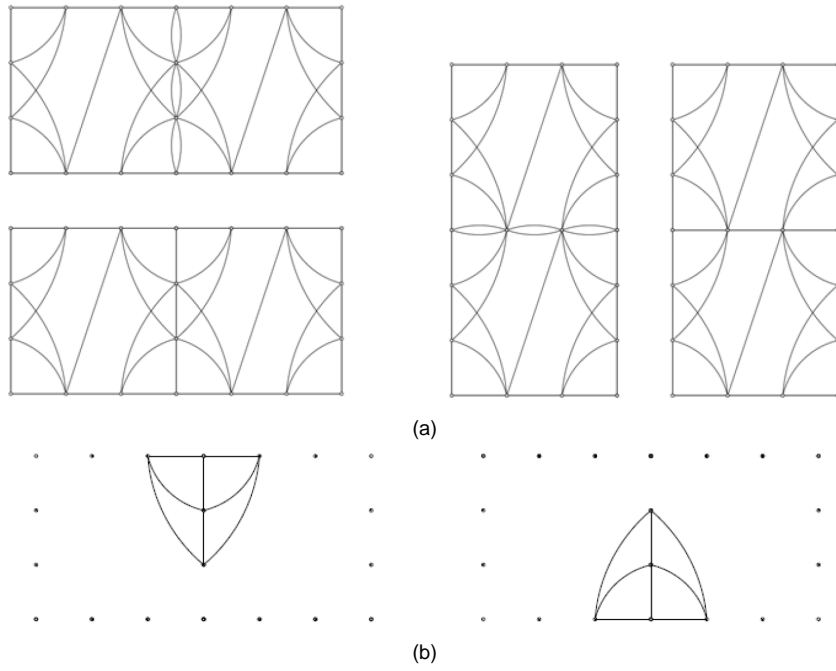


Fig. 4. (a) Subgraph corresponding to SESs of Type II, (b) Pattern of Type II self-equilibrating systems in horizontal direction.

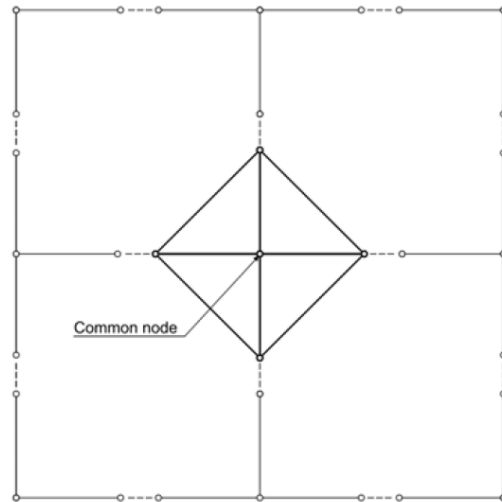


Fig. 5. The SES of Type III corresponding to the common node of four rectangular elements.

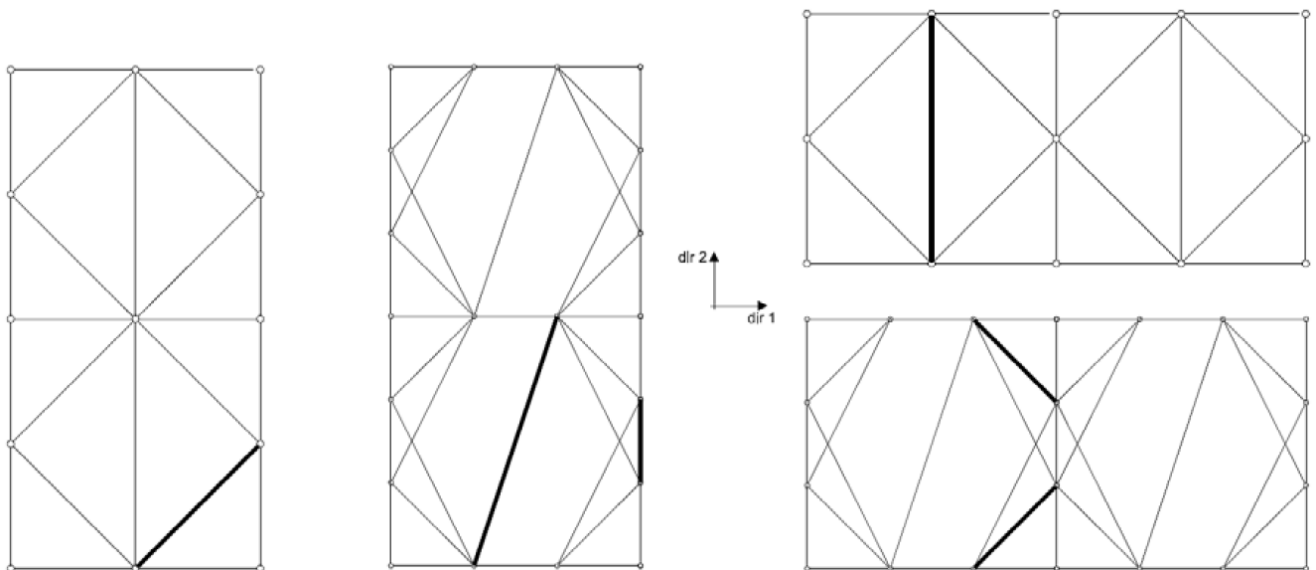


Fig. 6. Selected generators of the Type II SES.

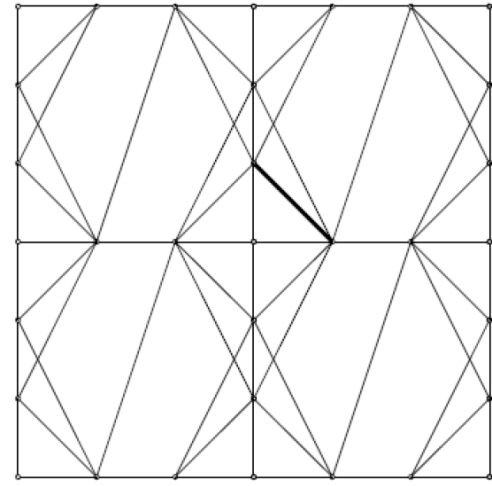
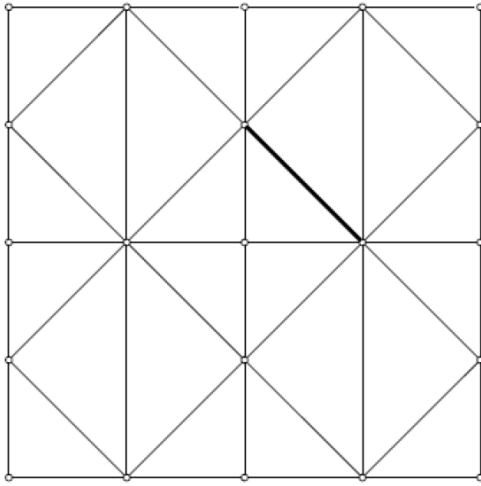


Fig. 7. Selected generators of the Type III SES.

For quadratic and rectangular element the generators of SESs Type II and Type III are illustrated in Fig. 6 and Fig. 7, respectively. It should be noted that the generators corresponding to Type I were chosen previously. In addition, the generators corresponding to an opening are the last non-zero entries of its columns which are not common with the previously selected generators.

Algorithm

Step 1: Generate the associate graph of the FEM and use an efficient method for its nodal numbering [30]. It is obvious that good numbering of this graph corresponds to good numbering of elements of the FEM. This numbering leads to a banded adjacency matrix of the graph and correspondingly to a banded flexibility matrix. Since the numbering of the members of the interface graphs corresponds to the element numbering of the finite elements, such a numbering is the only parameter for controlling the bandwidth of the flexibility matrix.

Step 2: Set up the equilibrium matrix of the FEM

Step 3: Generate the interface graph and perform its numbering. The numbering of this graph should be performed according to the element numbering of the considered FEM. After this numbering the interface graph can easily be formed and its members can be numbered.

Step 4: Find the Type I self-equilibrating systems. All multiple members of the interface graph are identified and the values -1 and 1 are assigned to appropriate rows (corresponding to the member numbers) and the corresponding minimal null vectors are created.

Step 5: Find the Type II self-equilibrating systems The $\frac{N}{4} - 1$ SESs of Type II should be extracted from two adjacent elements.

Step 6: Find the Type III self-equilibrating systems For each minimal cycle of natural associate graph of FEM with four members (one common node), one SES and with eight or more members (Opening), three SESs should be extracted.

Step 7: Order the null vectors. At this step the constructed null vectors should be ordered such that their last non-zero entries form a list with an ascending order.

7 Numerical examples

In this section three FEMs are considered, one of these models is assumed to be supported in statically indeterminate fashion and the other two supported in a determinate fashion. The effect of the presence of additional supports can separately be included for each special case with no difficulty as discussed in [32, 33]. The equilibrium matrices are formed. Null bases and the flexibility matrices are constructed and the required computational times, and the condition numbers are calculated. In all the following examples, mnz represents the number of non-zero entries and $\lambda_{\max}/\lambda_{\min}$ is the ratio of the extreme eigenvalues taken as the condition number of a matrix. The comparison between present algorithm and algebraic force method is shown in Tab. 4 for all three examples. Finally the present method is validated through comparison of resulting stresses using the present graph-theoretical force method and the displacement method.

7.1 Example 1

The lining of a tunnel is considered supported in a statically determinate manner, and its applied load is depicted in Fig. 8. This structure is discretized using rectangular 8-node finite elements. The properties of the model are as follows:

Poisson's ratio = 0.3

Elastic modulus $E = 2e+7 \text{ kN/m}^2$

Thickness $t = 1.00 \text{ m}$

Number of rectangular 8-node elements = 100

Number of nodes = 405

$DSI = 100 \times 13 - 2 \times 405 + 3 = 493$

Number of Type I self-equilibrating systems = 296 (60%)

Number of Type II self-equilibrating systems = 148 (30%)

Number of Type III self-equilibrating systems = 49 (10%)

The interface and natural associate graphs of the FEM model are illustrated in Fig. 9. The pattern of the equilibrium matrix is shown in Fig. 10. The sparsity of the final null basis obtained by the present method is approximately 6.7% of that of QR method and 6.07% of the LU method as depicted in Fig. 11. The flexi-

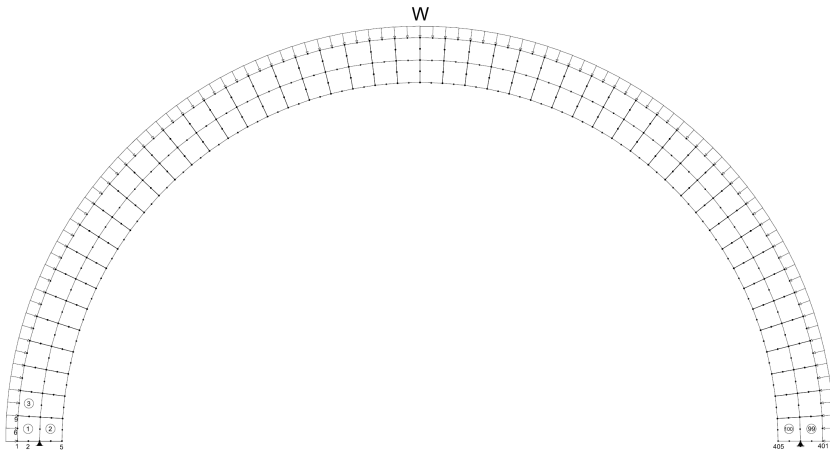
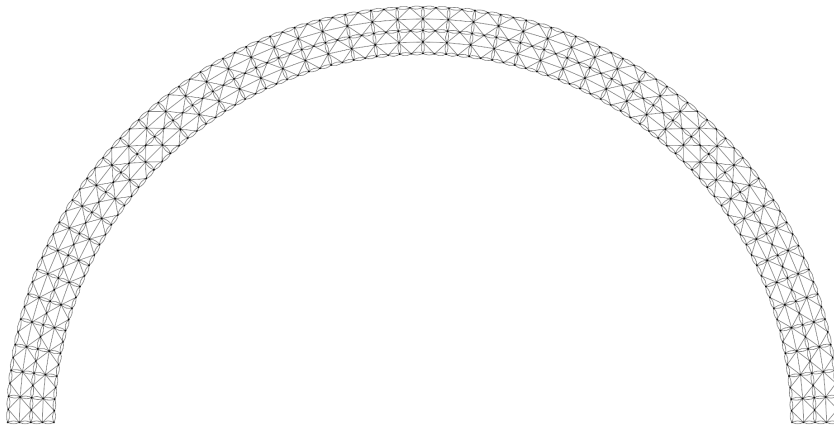
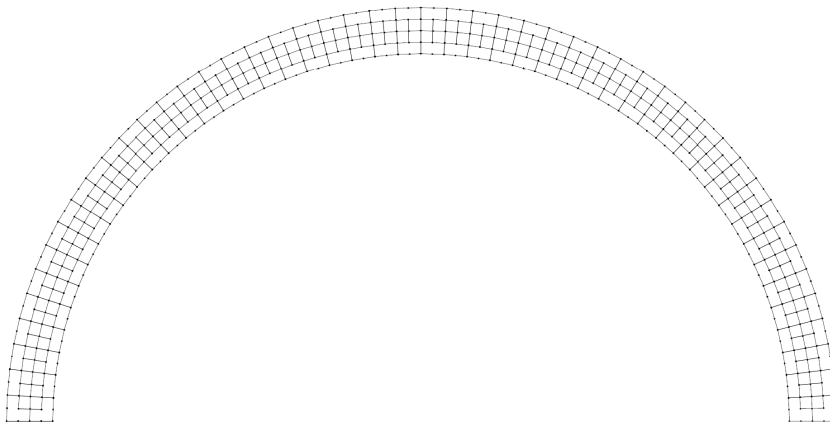


Fig. 8. A lining of a tunnel, the discretization and loading of the structure.



(a)



(b)

Fig. 9. Interface and natural associate graphs of Example 1, (a) Interface graph, (b) natural associate graph.

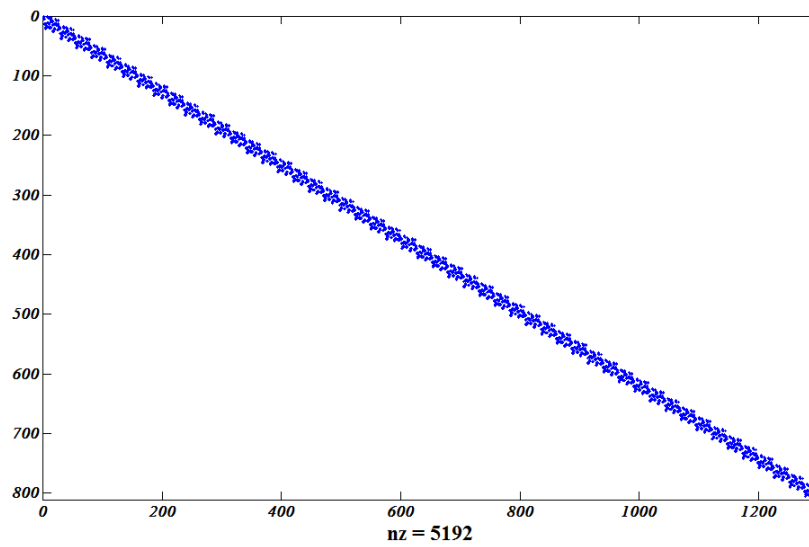


Fig. 10. Pattern of the equilibrium matrix for Example 1.

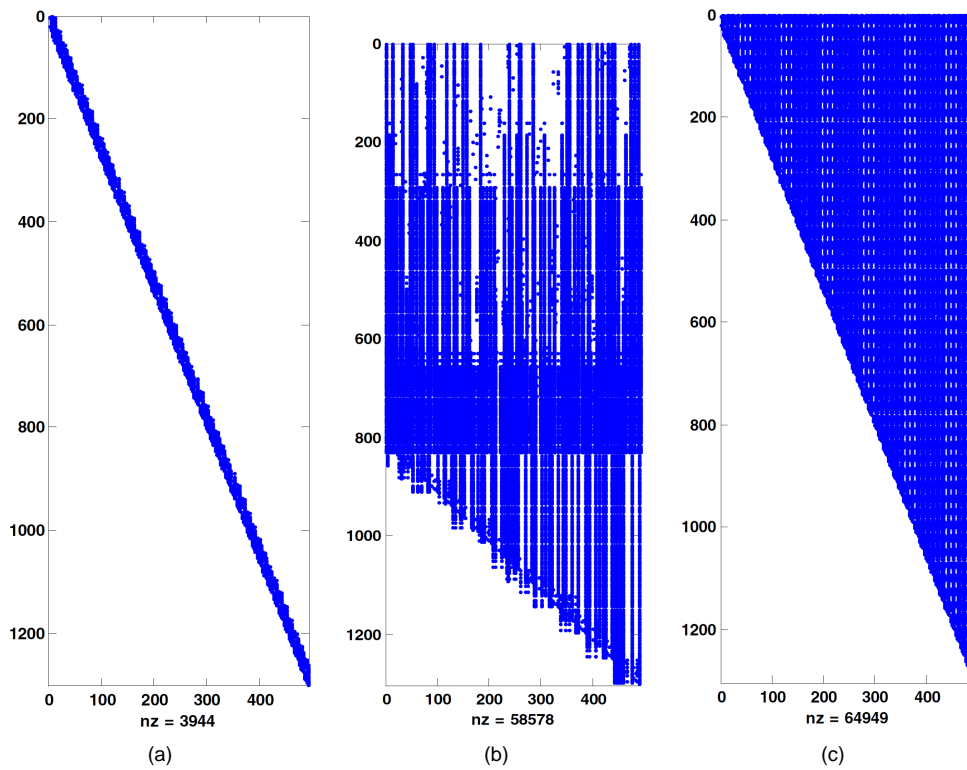


Fig. 11. Patterns and number of non-zero entries of the null bases of Example 1: (a) present algorithm, (b) QR factorization and (c) LU factorization.

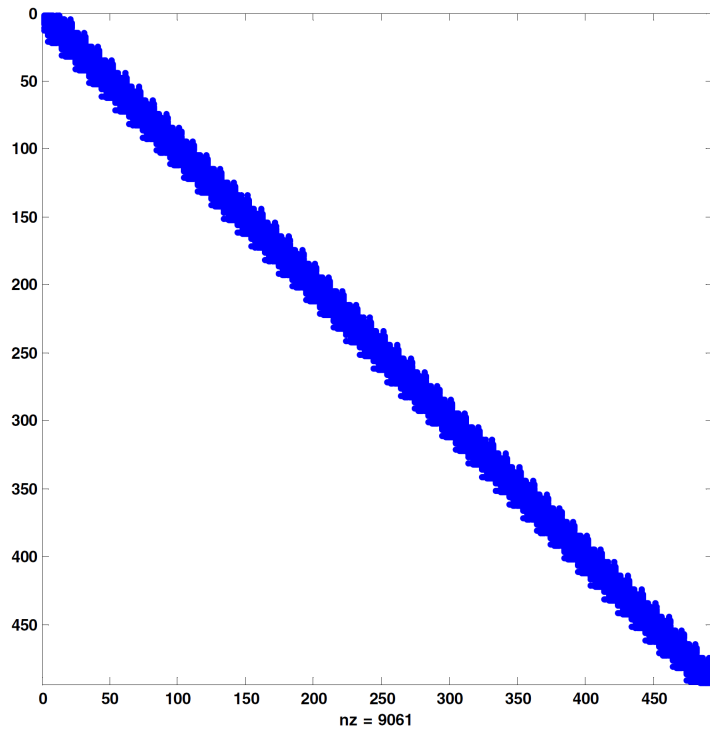


Fig. 12. Patterns of the flexibility matrix $G = \mathbf{B}_1' \mathbf{F}_m \mathbf{B}_1$ for Example 1 using the proposed method.

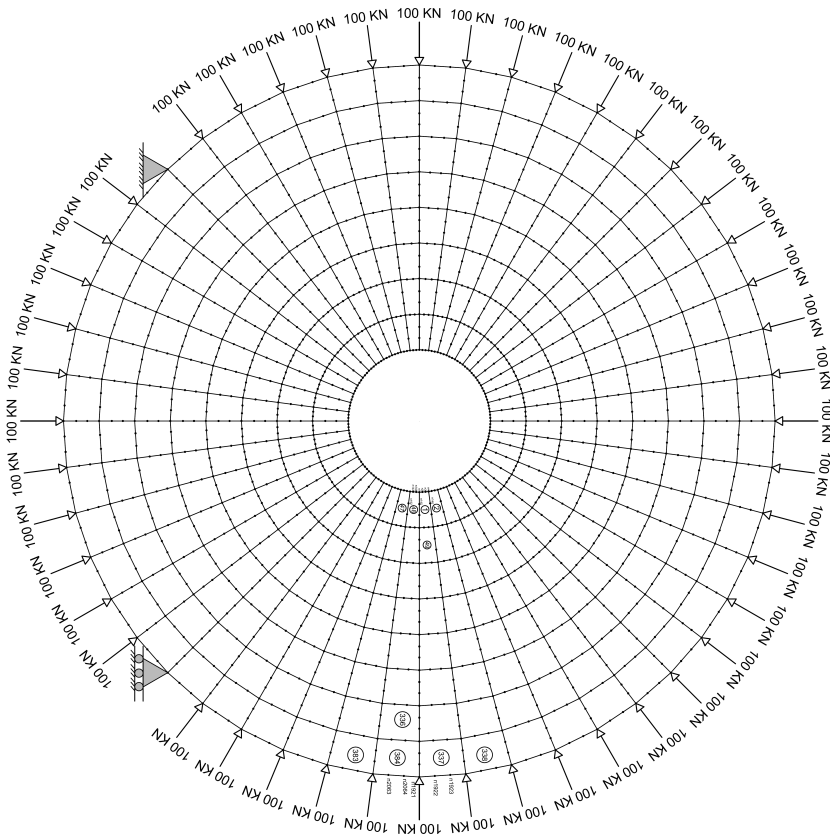


Fig. 13. A circulate plate with an opening.

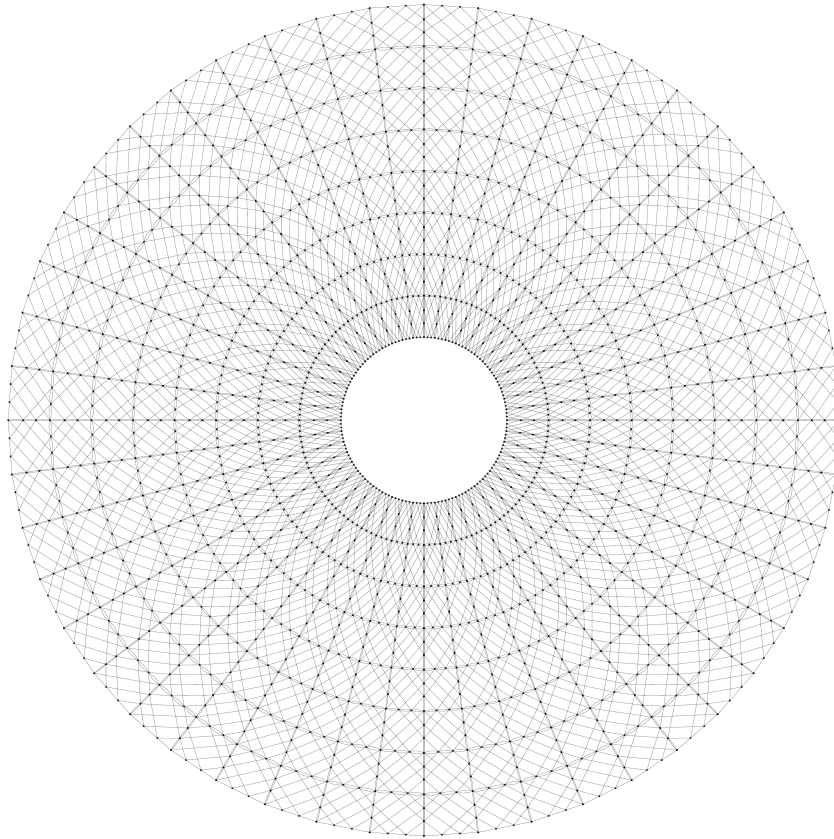


Fig. 14. The interface graph of Example 2.

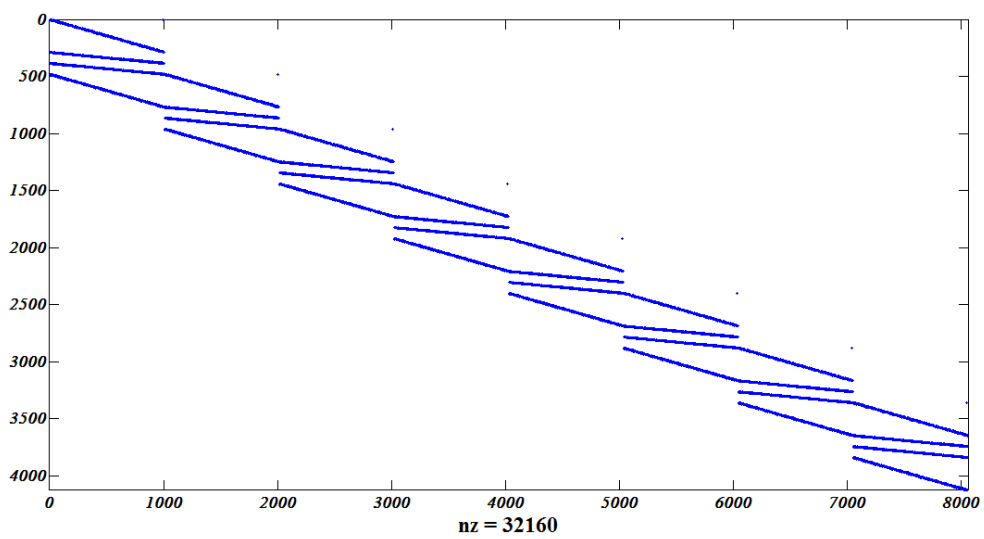


Fig. 15. Pattern of the equilibrium matrix for Example 2.

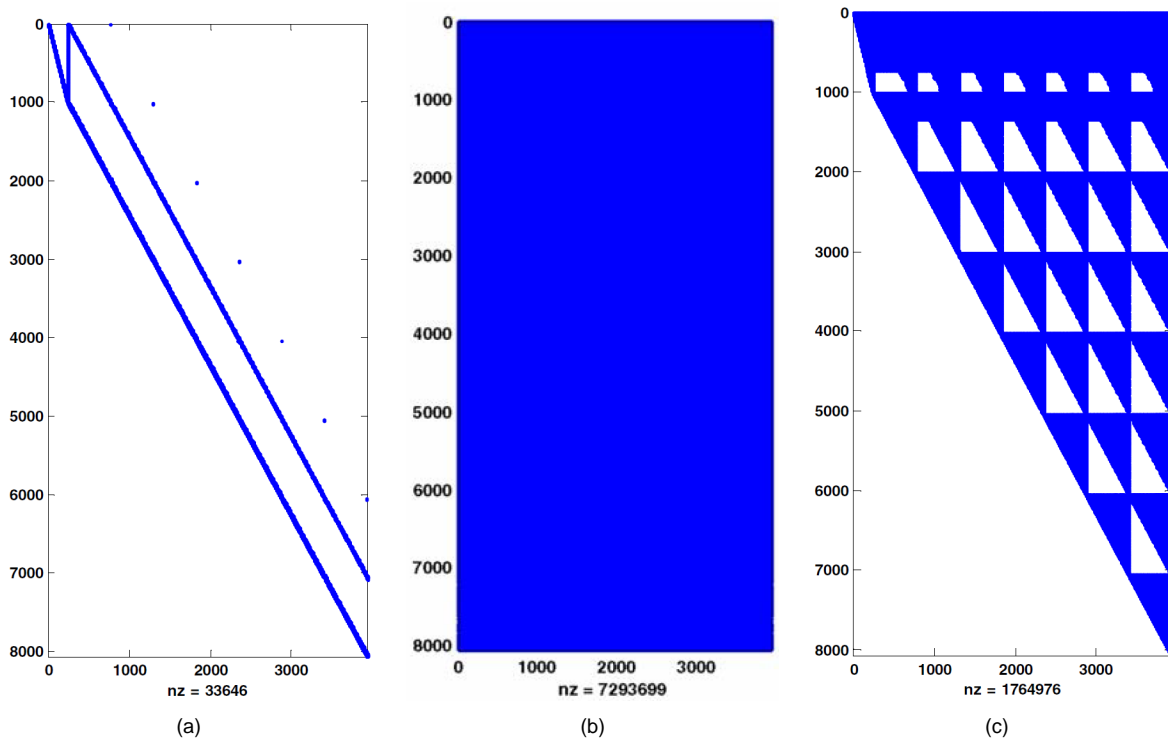


Fig. 16. Patterns and the number of non-zero entries of the null bases of Example 2: (a) present algorithm, (b) QR factorization and (c) LU factorization.

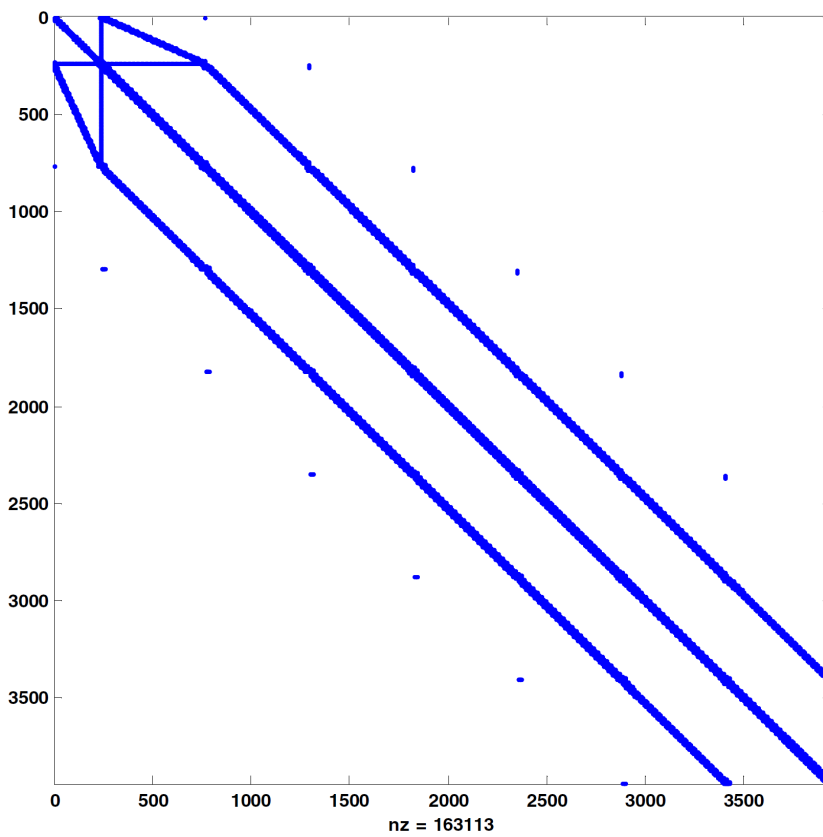


Fig. 17. Patterns of flexibility matrix $\mathbf{G} = \mathbf{B}_1^T \mathbf{F}_m \mathbf{B}_1$ for Example 2 using the proposed method.

bility matrix, G , is also well-structured as shown in Fig. 12. The results are verified by standard displacement method in Tab. 1.

7.2 Example 2

A circular plate and its applied load are shown in Fig. 13. The internal and external diameters are 1.00 m and 5.00 m, respectively. This structure is discretized using 12-node rectangular finite elements. The properties of the model are as follows:

Poisson's ratio = 0.3
Elastic modulus $E = 2e+7 \text{ kN/m}^2$
Thickness $t = 1.00 \text{ m}$
Number of rectangular 12-node elements = 384,
Number of nodes = 2064
$DSI = 384 \times 21 - 2 \times 2064 + 3 = 3939$
Number of Type I self-equilibrating systems = 2160 ($\approx 55\%$)
Number of Type II self-equilibrating systems = 1440 ($\approx 36\%$)
Number of Type III self-equilibrating systems = 336 (internal nodes) + 3 (an opening) = 339 ($\approx 8.5\%$)

The interface and natural associate graph of the FEM model is illustrated in Fig. 14 and Fig. 3. The pattern of the equilibrium matrix is shown in Fig. 15. The sparsity of the final null basis obtained by the present method is approximately 0.46% of the QR method and 1.9% of the LU approach as depicted in Fig. 16. The flexibility matrix is also well-structured as shown in Fig. 17. The results are verified by the standard displacement method in Tab. 2.

Tab. 1. Comparison of the displacement method and the present force method for Example 1.

Method	Element stresses					
	Displacement method			The present force method		
	σ_{xx}	σ_{yy}	σ_{xy}	σ_{xx}	σ_{yy}	σ_{xy}
Element	kN/cm^2			kN/cm^2		
1	-0.1806	-0.7815	0.2763	-0.1806	-0.7815	0.2763
10	-0.0918	-0.7379	-0.2186	-0.0918	-0.7379	-0.2186
20	-0.3097	-0.6082	-0.4040	-0.3097	-0.6082	-0.4040
30	-0.6168	-0.3721	-0.4470	-0.6168	-0.3721	-0.4470
40	-0.8943	-0.1416	-0.3060	-0.8943	-0.1416	-0.3060
50	-1.0196	-0.0346	-0.0306	-1.0196	-0.0346	-0.0306
60	-0.9346	-0.1073	0.2586	-0.9346	-0.1073	0.2586
70	-0.6790	-0.3214	0.4333	-0.6790	-0.3214	0.4333
80	-0.3672	-0.5666	0.4265	-0.3672	-0.5666	0.4265
90	-0.1244	-0.7240	0.2627	-0.1244	-0.7240	0.2627
100	-0.1361	-0.7739	0.3446	-0.1361	-0.7739	0.3446

7.3 Example 3

The FEM of a dam which is supported in a statically indeterminate fashion is depicted in Fig. 18. This structure is discretized using 8-node and 12-node rectangular finite elements separately. It should be noted that the number of support elements depends on the choice of 8 or 12 nodes per finite element. The properties of the models are:

Tab. 2. Comparison of the displacement method and the present force method for Example 2.

Method	Element stresses					
	Displacement method			The present force method		
	σ_{xx}	σ_{yy}	σ_{xy}	σ_{xx}	σ_{yy}	σ_{xy}
Element	kN/cm^2			kN/cm^2		
337	-2.6962	-2.8935	0.0188	-2.6962	-2.8935	0.0188
340	-2.7314	-2.8329	0.0701	-2.7314	-2.8329	0.0701
343	-2.7879	-2.7646	0.0793	-2.7879	-2.7646	0.0793
346	-2.8348	-2.7121	0.0464	-2.8348	-2.7121	0.0464
349	-2.8483	-2.6972	-0.0098	-2.8483	-2.6972	-0.0098
352	-2.8220	-2.7262	-0.0612	-2.8220	-2.7262	-0.0612
255	-2.7686	-2.7870	-0.0813	-2.7686	-2.7870	-0.0813
358	-2.7158	-2.8547	-0.0572	-2.7158	-2.8547	-0.0572
361	-2.6939	-2.9112	0.0059	-2.6939	-2.9112	0.0059
364	-2.7288	-2.9929	0.1074	-2.7288	-2.9929	0.1074
367	-0.8483	-2.4765	-0.0155	-0.8483	-2.4765	-0.0155
370	-2.4803	-2.7025	-0.0552	-2.4803	-2.7025	-0.0552
373	-2.5319	-2.7105	0.0084	-2.5319	-2.7105	0.0084
376	-2.3806	-2.6839	0.0927	-2.3806	-2.6839	0.0927
379	-2.6693	-2.7841	-0.4591	-2.6693	-2.7841	-0.4591
382	-2.7092	-2.9526	-0.0679	-2.7092	-2.9526	-0.0679

Poisson's ratio = 0.3
Elastic modulus $E = 2e+7 \text{ kN/m}^2$
Thickness $t = 1.00 \text{ m}$
Case 1: Number of rectangular 8-node elements = 192,
Number of nodes = 681
Case 2: Number of rectangular 12-node elements = 192,
Number of nodes = 1117
$DSI_{8\text{-node}} = 192 \times 13 - 2 \times 681 + 82 = 1216$
$DSI_{12\text{-node}} = 192 \times 21 - 2 \times 1117 + 122 = 1920$
Number of Type I self-equilibrating systems,
Case 1 = 664 (58.5%)
Number of Type II self-equilibrating systems,
Case 1 = 332 (29%)
Number of Type III self-equilibrating systems,
Case 1 = 141 (12.5%)
Number of Type I self-equilibrating systems,
Case 2 = 996 (55%)
Number of Type II self-equilibrating systems,
Case 2 = 664 (36.8%)
Number of Type III self-equilibrating systems,
Case 2 = 141 (8.2%)

The interface and natural associate graphs of the FEM model are illustrated in Fig. 19 for FEM with 8-node elements. The interface graph for other cases can simply be obtained. The final null basis obtained for both cases by the present method are depicted in Fig. 20 and Fig. 21. The flexibility matrix is also well-structured as shown in Fig. 22. The results are verified by the standard displacement method in Tab. 3.

Tab. 3. The comparison of the displacement method and the present force method for Example 3.

Method	Element Stresses											
	8-node						12-node					
	Displacement method			The present force method			Displacement method		The present force method			
	σ_{xx}	σ_{yy}	σ_{xy}	σ_{xx}	σ_{yy}	σ_{xy}	σ_{xx}	σ_{yy}	σ_{xy}	σ_{xx}	σ_{yy}	σ_{xy}
Element	kN/cm^2						kN/cm^2					
8	0.0560	0.9029	0.0436	0.0560	0.9029	0.0436	0.0322	0.8158	0.0426	0.0322	0.8158	0.0426
16	-0.0430	-1.0513	-0.2987	-0.0430	-1.0513	-0.2987	0.0346	-0.6760	-0.3087	0.0346	-0.6760	-0.3087
24	0.2060	0.0529	-0.0512	0.2060	0.0529	-0.0512	0.2399	0.1925	-0.0526	0.2399	0.1925	-0.0526
32	0.0655	1.4381	0.1071	0.0655	1.4381	0.1071	0.1210	1.6845	0.0629	0.1210	1.6845	0.0629
40	-1.0339	-1.4361	-0.9329	-1.0339	-1.4361	-0.9329	-0.9501	-1.1784	-0.9567	-0.9501	-1.1784	-0.9567
48	0.0694	0.0060	0.0006	0.0694	0.0060	0.0006	0.0736	0.0340	0.0035	0.0736	0.0340	0.0035
56	-0.1939	1.2847	0.0540	-0.1939	1.2847	0.0540	-0.1916	1.2772	0.0490	-0.1916	1.2772	0.0490
64	-0.1546	1.1539	-0.0439	-0.1546	1.1539	-0.0439	-0.1572	1.1521	-0.0411	-0.1572	1.1521	-0.0411
72	-0.1114	1.0027	-0.0788	-0.1114	1.0027	-0.0788	-0.1124	1.0021	-0.0764	-0.1124	1.0021	-0.0764
80	-0.0979	0.8474	-0.0779	-0.0979	0.8474	-0.0779	-0.0975	0.8475	-0.0767	-0.0975	0.8475	-0.0767
88	-0.0891	0.6999	-0.0703	-0.0891	0.6999	-0.0703	-0.0884	0.7002	-0.0695	-0.0884	0.7002	-0.0695
96	-0.0809	0.5645	-0.0616	-0.0809	0.5645	-0.0616	-0.0802	0.5648	-0.0608	-0.0802	0.5648	-0.0608
104	-0.0729	0.4431	-0.0527	-0.0729	0.4431	-0.0527	-0.0722	0.4434	-0.0521	-0.0722	0.4434	-0.0521
112	-0.0650	0.3363	-0.0441	-0.0650	0.3363	-0.0441	-0.0643	0.3366	-0.0436	-0.0643	0.3366	-0.0436
120	-0.0570	0.2446	-0.0359	-0.0570	0.2446	-0.0359	-0.0564	0.2449	-0.0354	-0.0564	0.2449	-0.0354
128	-0.0491	0.1683	-0.0281	-0.0491	0.1683	-0.0281	-0.0485	0.1686	-0.0278	-0.0485	0.1686	-0.0278
136	-0.0412	0.1073	-0.0210	-0.0412	0.1073	-0.0210	-0.0407	0.1075	-0.0207	-0.0407	0.1075	-0.0207
144	-0.0333	0.0612	-0.0145	-0.0333	0.0612	-0.0145	-0.0329	0.0614	-0.0143	-0.0329	0.0614	-0.0143
152	-0.0254	0.0294	-0.0089	-0.0254	0.0294	-0.0089	-0.0251	0.0296	-0.0088	-0.0251	0.0296	-0.0088
160	-0.0176	0.0104	-0.0044	-0.0176	0.0104	-0.0044	-0.0173	0.0105	-0.0044	-0.0173	0.0105	-0.0044
168	-0.0097	0.0019	-0.0012	-0.0097	0.0019	-0.0012	-0.0096	0.0020	-0.0012	-0.0096	0.0020	-0.0012

Tab. 4. The comparison between present algorithm and algebraic force method for all three examples.

Example	Computational Time	Condition Number	$\frac{\lambda_{max}}{\lambda_{min}}$	Norms $\max \mathbf{A} \times \mathbf{B}_1 $	
		(Flexibility matrices)		Present	LU
	LU Time	Present Method	LU Factorization	Method	Factorization
Tunnel lining	1.21	47.65	1.63e+5	1.08e-15	4.04e-14
Circulate Beam	0.45	9.38e+5	8.73e+7	5.51e-14	1.76e-13
Retaining wall (8-node)	0.84	2.68e+4	4.28e+7	7.43e-12	2.67e-13
Retaining wall (12-node)	0.78	3.59e+5	8.01e+7	1.22e-13	1.90e-13

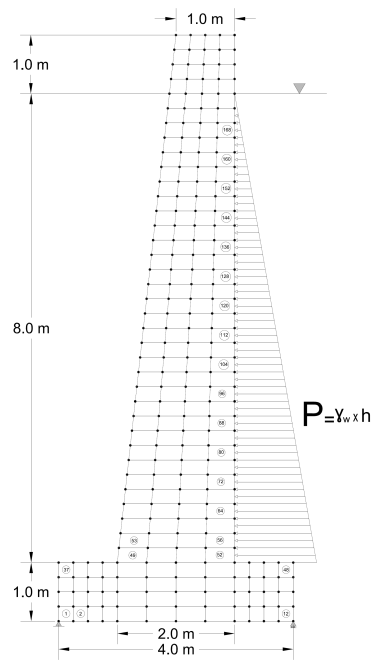


Fig. 18. A retaining wall and the corresponding rectangular meshes.

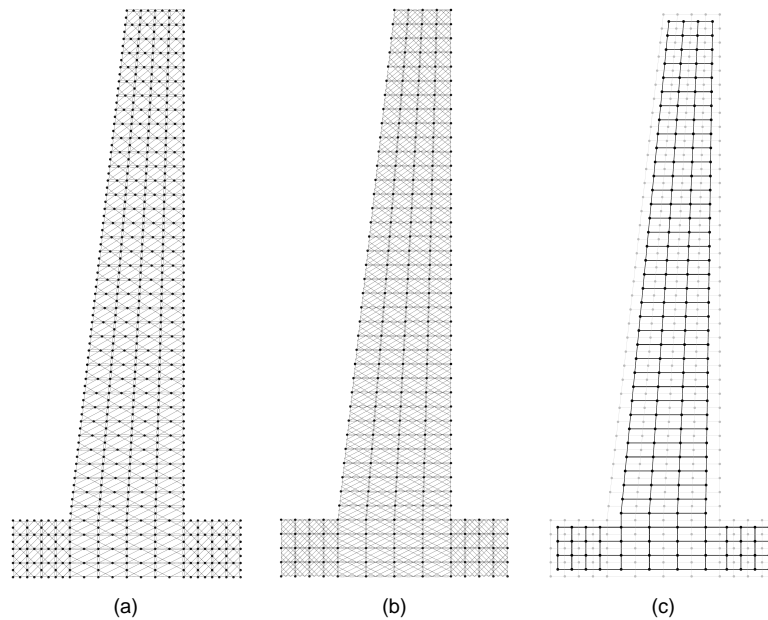


Fig. 19. Interface graph and natural associate graph for both cases of Example 3, (a) Interface graph for 8-node element, (b) Interface graph for 12-node element and (c) Associate graph for both cases.

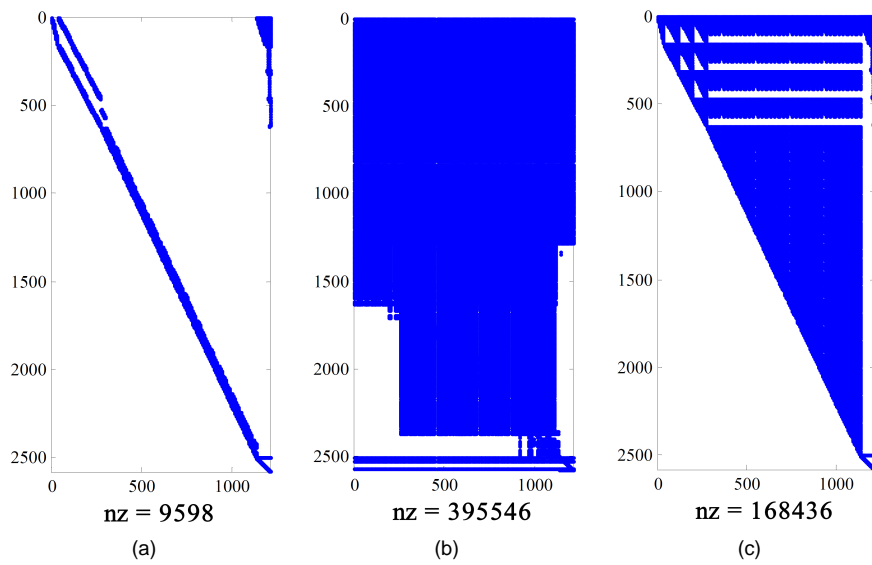


Fig. 20. Patterns and number of non-zero entries of null bases of Example 3 (8-node element): (a) present algorithm, (b) *QR* factorization and (c) *LU* factorization.

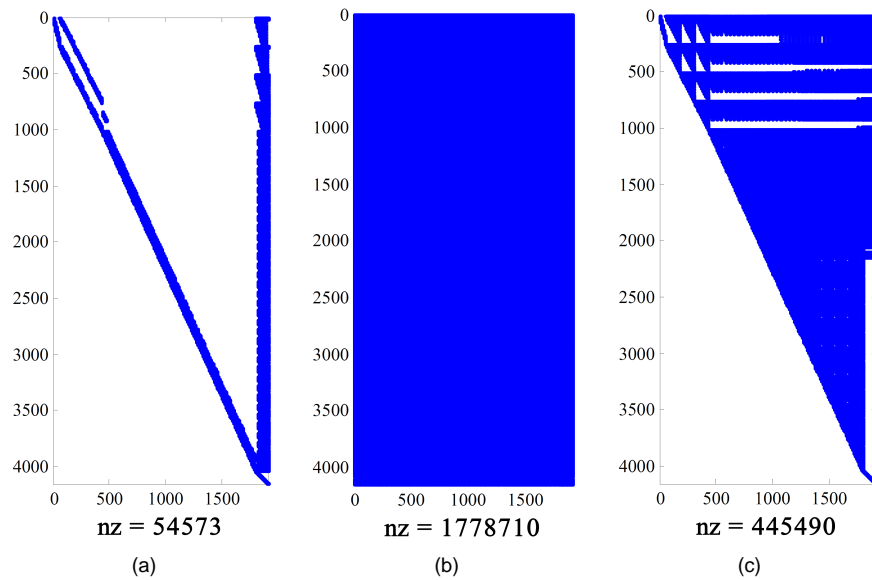


Fig. 21. Patterns and number of non-zero entries of null bases of Example 3 (12-node element): (a) present algorithm, (b) *QR* factorization and (c) *LU* factorization.

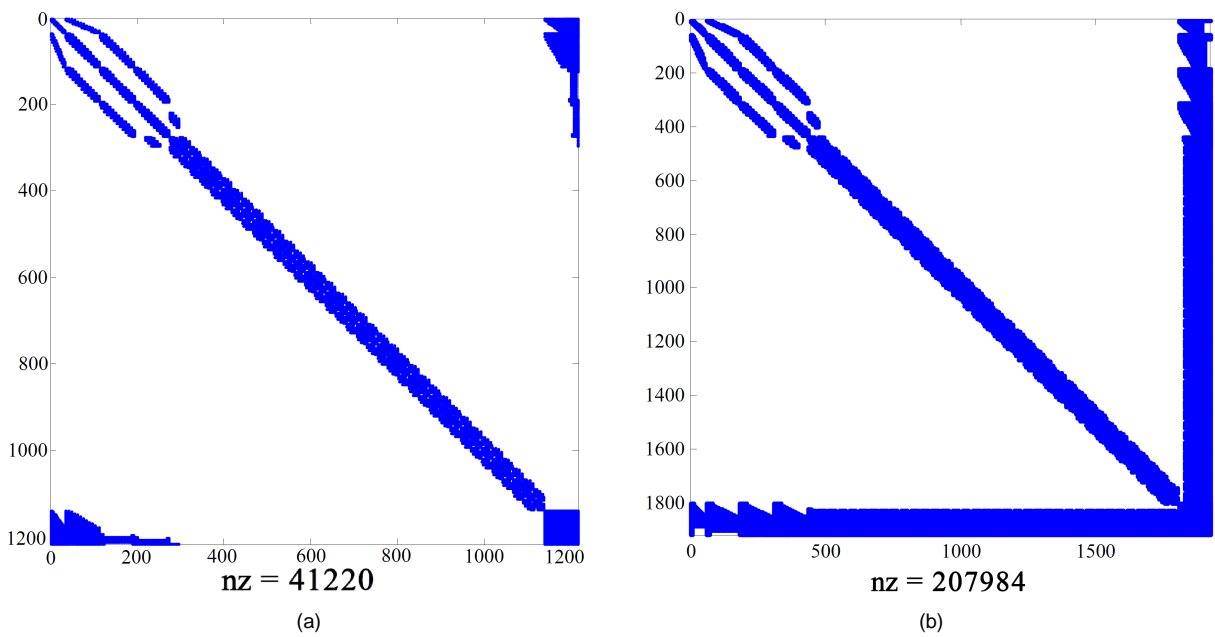


Fig. 22. Patterns of flexibility matrix $\mathbf{G} = \mathbf{B}_1^T \mathbf{F}_m \mathbf{B}_1$ of Example 3, (a) 8-node element, (b) 12-node element.

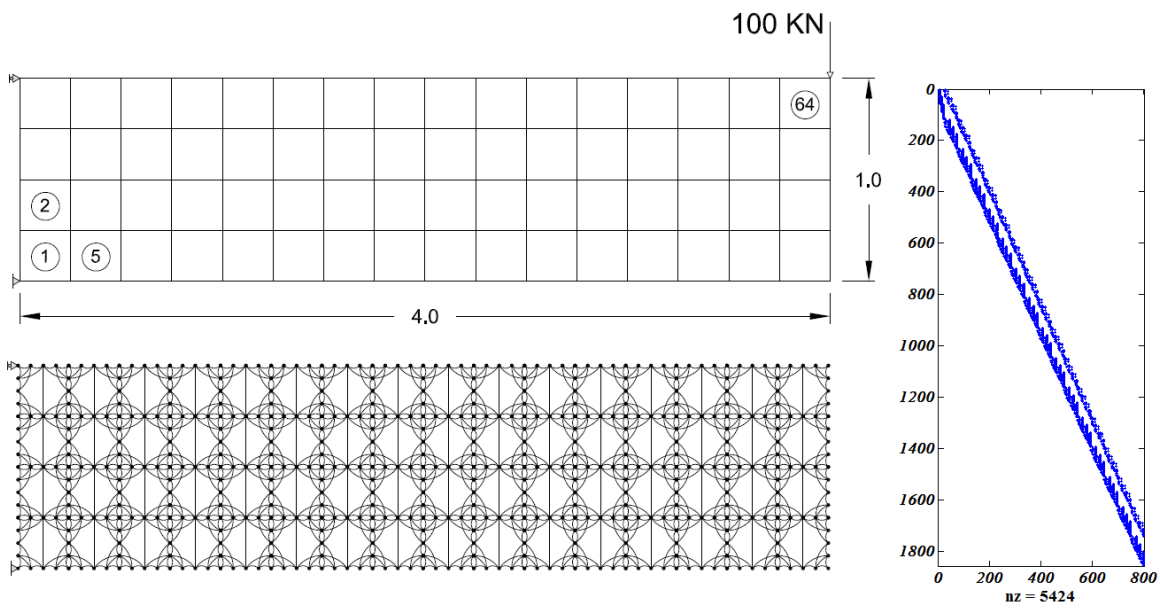


Fig. 23. A beam with 16-node rectangular elements, its corresponding interface graph and null vector matrix.

8 Concluding remarks

The main conclusions of this paper are as follows:

Solution of many examples reveals that good accuracy can be achieved by the present algorithm as shown in Tab. 4.

- Flexibility matrices obtained are highly sparse with narrowly banded. This is due to the use of regional cycles of the natural associate graphs and appropriate ordering of the selected self-equilibrating systems.
- The conditioning of the flexibility matrices generated by the present algorithm is better than those formed by the *LU* method as illustrated is Tab. 4.
- Because of a high reduction in the number of floating point operations, the resulted null basis has better accuracy in comparison to other methods. This is obvious, since nearly 60% of the null vectors are selected without numerical analysis and the remaining null vectors are obtained with working on small and limited lists.
- The method developed in this paper can easily be extended to FEMs with higher-order two-dimensional rectangular elements. For example, a beam which is discretized using 16-node elements is depicted in Fig. 23. The corresponding interface graph and null basis matrix are illustrated in Fig. 23. It should be noted that in the present method the most important point is selecting independent element forces system.
- The required computational time for the present method is considerably lower than those of the algebraic methods. Since the complexity of the *LU* method is $O(n^3)$, if the DSI of the model increases, then the time difference dramatically rises.
- In the present method, numbering the nodes of a finite element model is less important and only a suitable ordering of the members of the natural associate graph is required for reducing the bandwidth of the flexibility matrices.

Acknowledgement

The first author is grateful to the Iran National Science Foundation for the support.

References

- 1 **Henderson JdC**, *Topological aspects of structural analysis*, Aircraft Engineering, **32**, (1960), 137–141.
- 2 **Maunder E**, *Topological and linear analysis of skeletal structures*, PhD Thesis, London University, 1971.
- 3 **de Henderson JCC, Maunder EAW**, *A problem in applied topology: on the selection of cycles for the flexibility analysis of skeletal structures*, IMA Journal of Applied Mathematics, **5**(2), (1969), 254–269, DOI 10.1093/ima-mat/5.2.254.
- 4 **Kaveh A**, *Application of topology and matroid theory to the analysis of structures*, PhD Thesis, London University, 1974.
- 5 **Kaveh A**, *Improved cycle bases for the flexibility analysis of structures*, Computer Methods in Applied Mechanics and Engineering, **9**(3), (1976), 267–272, DOI 10.1016/0045-7825(76)90031-1.
- 6 **Kaveh A**, *A combinatorial optimization problem Optimal generalized cycle bases*, Computer Methods in Applied Mechanics and Engineering, **20**(1), (1979), 39–52, DOI 10.1016/0045-7825(79)90057-4.
- 7 **Cassell AC**, *An alternative method for finite element analysis; a combinatorial approach to the flexibility method*, Proceedings of the Royal Society A: Mathematical, Physical and Engineering Sciences, **352**(1668), (1976), 73–89, DOI 10.1098/rspa.1976.0164.
- 8 **Denke PH**, *A general digital computer analysis of statically indeterminate structures*, NASA-TD-D-, **1666**, (1962), 0–0.
- 9 **Robinson J**, *Integrated Theory of Finite Element Methods*, Wiley; New York, 1973.
- 10 **Topcu A**, *A contribution to the systematic analysis of finite element structures using the force method*, PhD Thesis, Essen University, 1979.
- 11 **Kaneko I, Lawo M, Thierauf G**, *On computational procedures for the force methods*, International Journal for Numerical Methods in Engineering, **18**(10), (1982), 1469–1495, DOI 10.1002/nme.1620181004.
- 12 **Soyer E, Topcu A**, *Sparse self-stress matrices for the finite element force method*, International Journal for Numerical Methods in Engineering, **50**(9), (2001), 2175–2194, DOI 10.1002/nme.119.
- 13 **Gilbert JR, Heath MT**, *Computing a sparse basis for the nullspace*, SIAM Journal on Algebraic Discrete Methods, **8**(3), (1986), 446–459, DOI 10.1137/0608037.
- 14 **Coleman TF, Pothen A**, *The null space problem I; complexity*, SIAM Journal on Algebraic Discrete Methods, **7**(4), (1986), 527–537, DOI 10.1137/0607059.
- 15 **Coleman TF, Pothen A**, *The null space problem II; complexity*, SIAM Journal on Algebraic Discrete Methods, **8**(4), (1987), 544–561, DOI 10.1137/0608045.
- 16 **Pothen A**, *Sparse null basis computation in structural optimization*, NumerischeMathematik., **55**, (1989), 501–519.
- 17 **Heath MT, Plemmons R, Ward J**, *Sparse orthogonal schemes for structural optimization using the force method*, SIAM Journal on Scientific and Statistical Computing, **5**(3), (1984), 514–532, DOI 10.1137/0905038.
- 18 **Patnaik SN**, *An integrated force method for discrete analysis*, International Journal for Numerical Methods in Engineering, **6**(2), (1973), 237–251, DOI 10.1002/nme.1620060209.
- 19 **Patnaik SN, Berke L, Gallagher RH**, *Integrated force method versus displacement method for finite element analysis*, Computers and Structures, **38**(4), (1991), 377–407, DOI 10.1016/0045-7949(91)90037-M.
- 20 **Csebfalvi A**, *Hybrid meta-heuristic method for continuous engineering optimization*, Periodica Polytechnica Civil Engineering, **53**(2), (2009), 93–100, DOI 10.3311/pp.ci.2009-2.05.
- 21 **Kaveh A, Massoudi MS**, *Efficient finite element analysis by graph-theoretical force method; rectangular and triangular plate bending elements*, Scientia Iranica, **18**(5), (2011), 1045–1053, DOI 10.1016/j.scient.2011.09.006.
- 22 **Kaveh A, Koohestani K**, *An efficient graph-theoretical force method for three-dimensional finite element analysis*, Communications in Numerical Methods in Engineering, **24**(11), (2008), 1533–1551, DOI 10.1002/cnm.1051.
- 23 **Kaveh A, Tolou Kian MJ**, *Efficient finite element analysis using graph-theoretical force method with brick elements*, Finite Elements for Analysis and Design, **54**, (2012), 1–15, DOI 10.1016/j.finel.2012.01.002.
- 24 **Kaveh A, Naseri Nasab E**, *A four-node quadrilateral element for finite element analysis via an efficient force method*, Asian Journal of Civil Engineering, **10**, (2009), 283–307.
- 25 **Kaveh A, Naseri Nasab E**, *A new four-node quadrilateral plate bending element for highly sparse and banded flexibility matrices*, Acta Mechanica, **209**(3-4), (2010), 295–309, DOI 10.1007/s00707-009-0180-5.
- 26 **Przemieniecki JS**, *Theory of Matrix Structural Analysis*, McGraw-Hill, 1968.

- 27 **Kurutz M.** *Stability of equilibrium and compatibility of structures with uniaxial material behavior*, Periodica Polytechnica Civil Engineering, **38/4**, (1994), 415–430.
- 28 **Kaveh A, Roosta GR.** *Comparative study of finite element nodal ordering methods*, Engineering Structures, **20**(1-2), (1998), 86–96, DOI 10.1016/S0141-0296(97)00047-3.
- 29 **Kaveh A, Beheshti S.** *Weighted triangular and circular graph products for configuration processing*, Periodica Polytechnica Civil Engineering, **56/1**, (2012), 1–9.
- 30 **Kaveh A.** *Structural Mechanics: Graph and Matrix Methods*, 3rd edition, Research Studies Press (Wiley); Somerset UK, 2004.
- 31 **Kaveh A.** *Computational Structural Analysis and Finite Element Methods*, 3rd edition, Springer Cham; Somerset UK, 2014, DOI 10.1007/978-3-319-02964-1.
- 32 **Kaveh A, Fazli H.** *Analysis of frames by structuring technique based on using algebraic and graph methods*, Communications in Numerical Methods in Engineering, **23**, (2007), 921–943.
- 33 **Kaveh A, Koohestani K, Taghizadeh N.** *Force method for finite element models with indeterminate support conditions*, Asian Journal of Civil Engineering, **8**, (2007), 403–417.

Appendix: Index

FEM	Finite element model
SES	Self-equilibrating system
A	Equilibrium matrix
B₁	Self-stress matrix
F_m	Unassembled flexibility matrix
N	Number of nodes of FEM
M	Number of elements of FEM (the number of members of the Natural associate graph)
IG	Interface graph
NAG	Natural associate graph
Type I self-equilibrating system	Self-equilibrium system which is constructed on a 2-multiple member
Type II self-equilibrating system	Self-equilibrium system which is extracted from two adjacent elements of FEM
Type III self-equilibrating system	Self-equilibrium system which is extracted from cycle of the NAG
DSI	Degree of statical indeterminacy
M'	Number of members of the associate graph of the model